



Supplement of

Variability in sediment particle size, mineralogy, and Fe mode of occurrence across dust-source inland drainage basins: the case of the lower Drâa Valley, Morocco

Adolfo González-Romero et al.

Correspondence to: Adolfo González-Romero (agonzal3@bsc.es) and Xavier Querol (xavier.querol@idaea.csic.es)

The copyright of individual parts of the supplement might differ from the article licence.

SUPPLEMENTARY MATERIAL

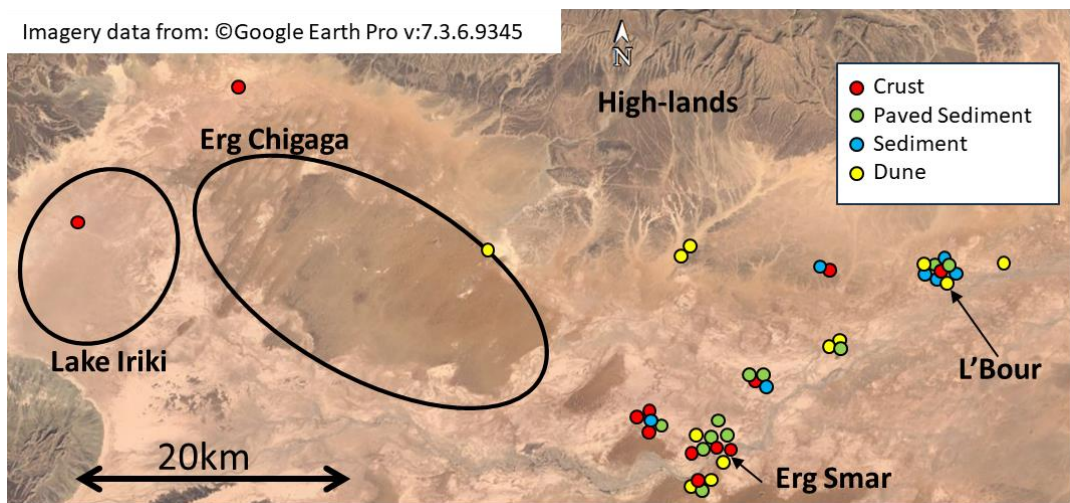


Figure S1. Map of the samples at the Lower Drâa Basin, S. Morocco. Type of samples: red dots: crusts, green dots: paved sediments, blue dots: sediments and yellow dots: dunes. Position is approximate for a better visualization of the samples.

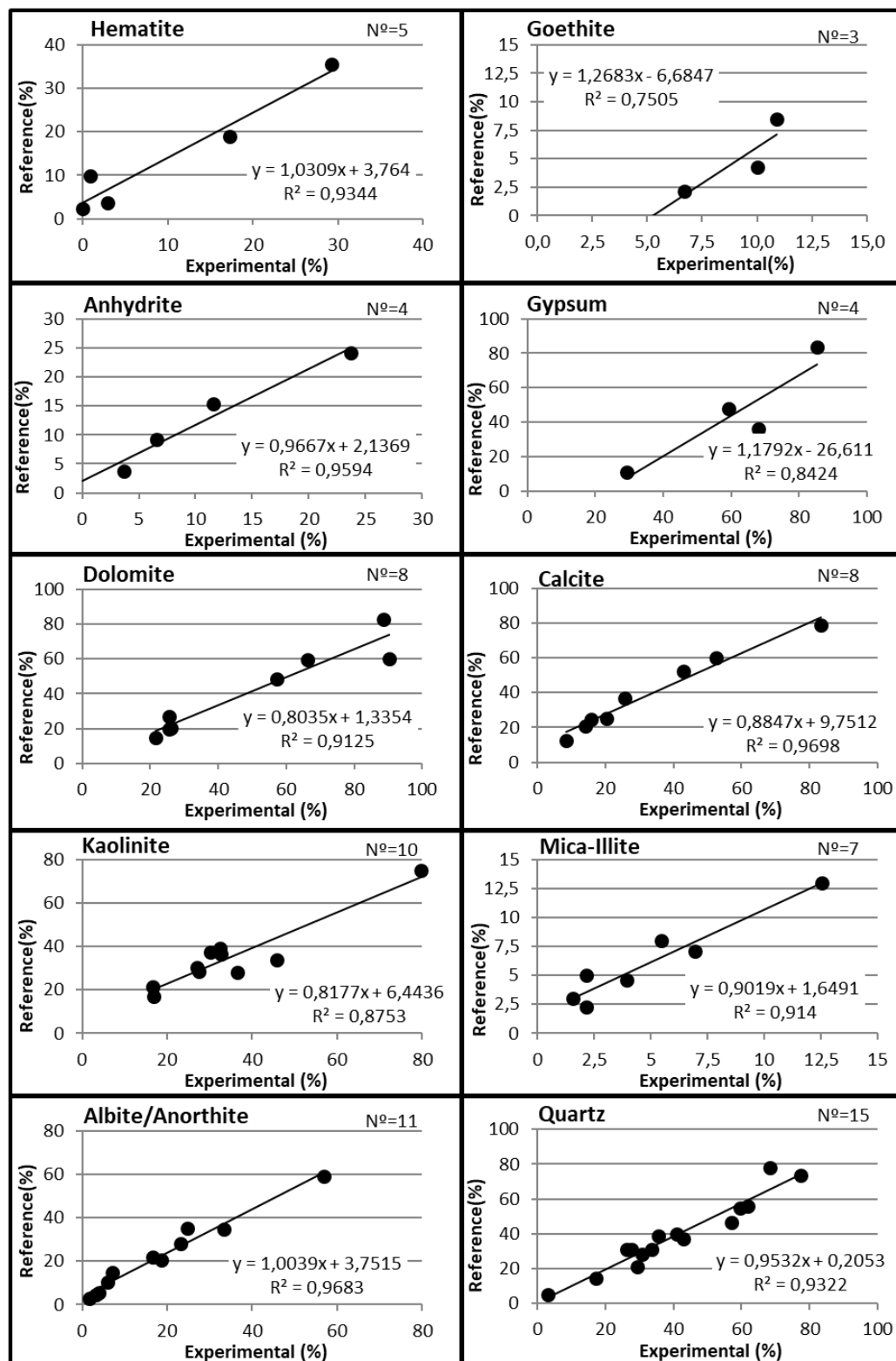


Figure S2. Cross correlation analysis of the content of minerals in mixtures of reference materials and the results obtained by using the internal reference method in this study. R², the regression equation and the number of samples analysed are represented on the graphic. All the values are % of mineral in mass.

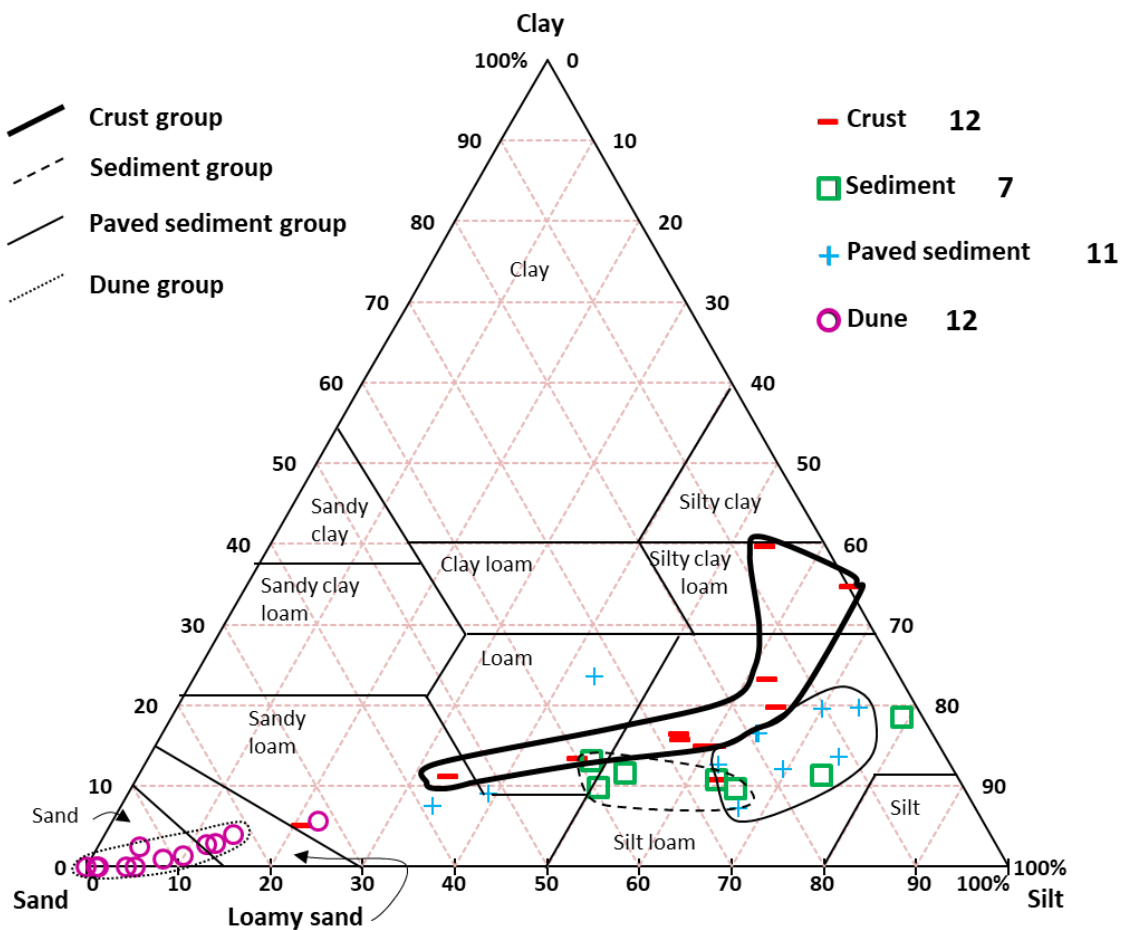


Figure S3. Ternary diagram for sand, silt and clay fractions, extracted from Valentin and Bresson (1992). Samples are differentiated by marker types and grouped with line types. Numbers in the legend indicate the number of samples represented in every group.

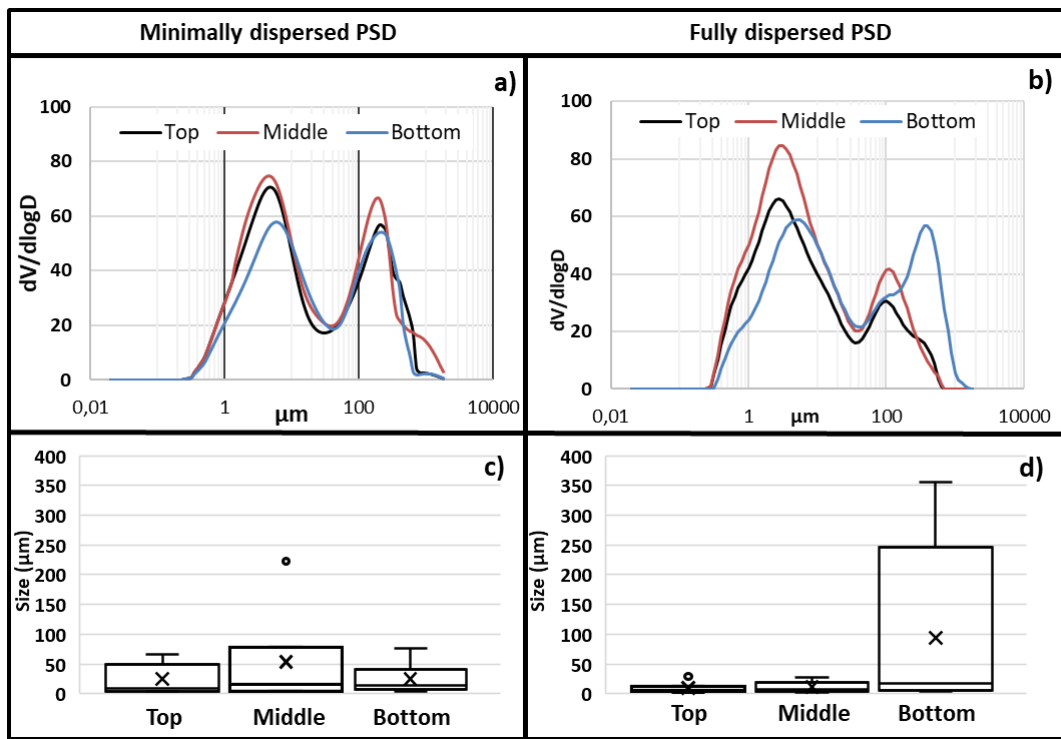


Figure S4. (a) MDP PSD and (b) FDP PSD from top, middle and bottom sections of crusts; Mean particle size median diameter from c) FDP PSD and d) MDP PSD.

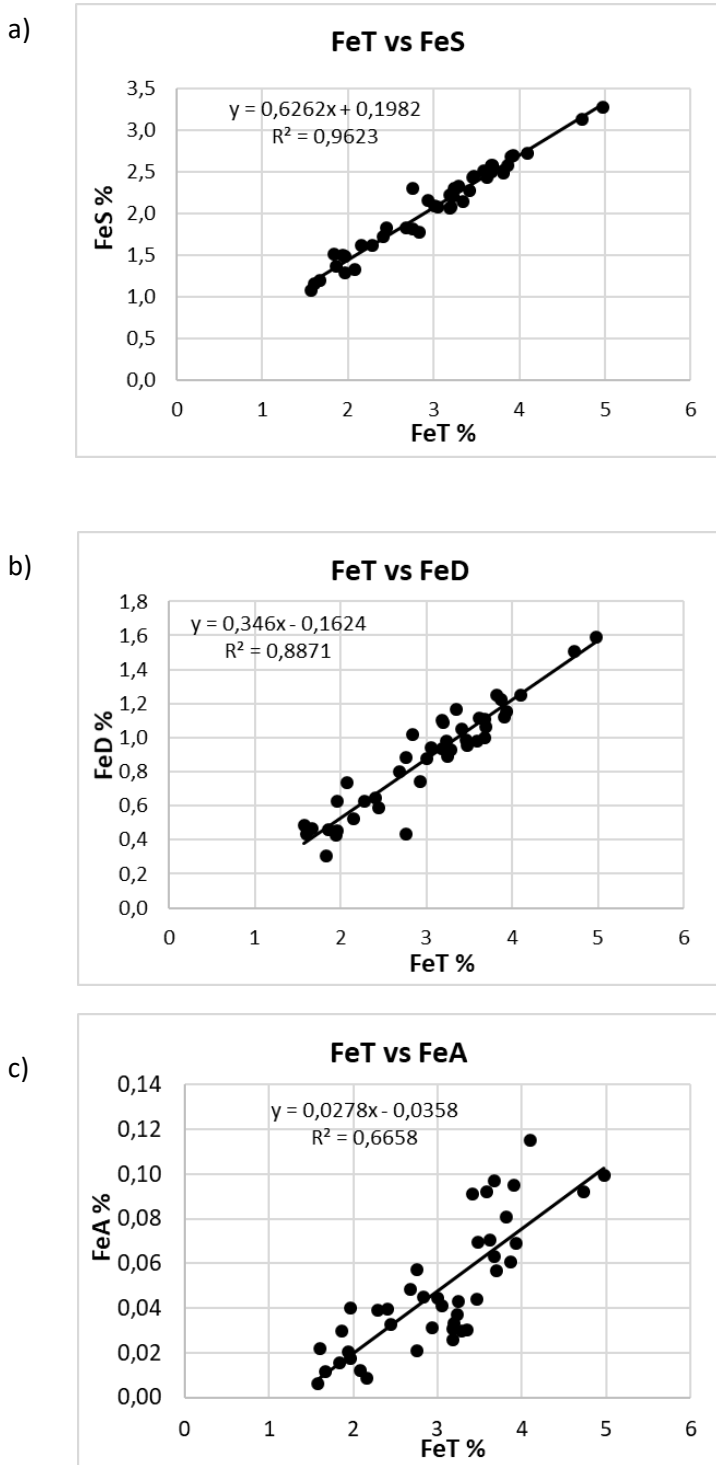


Figure S5. Linear correlations between FeS (structural iron in minerals like clays) a), FeD (iron in minerals like hematite and goethite) b) and FeA (iron adsorbed in clays and nanosized Ferrihydrite ($\text{Fe}_{4-5}(\text{OH},\text{O})_{12}$) c) and FeT (Total iron content).

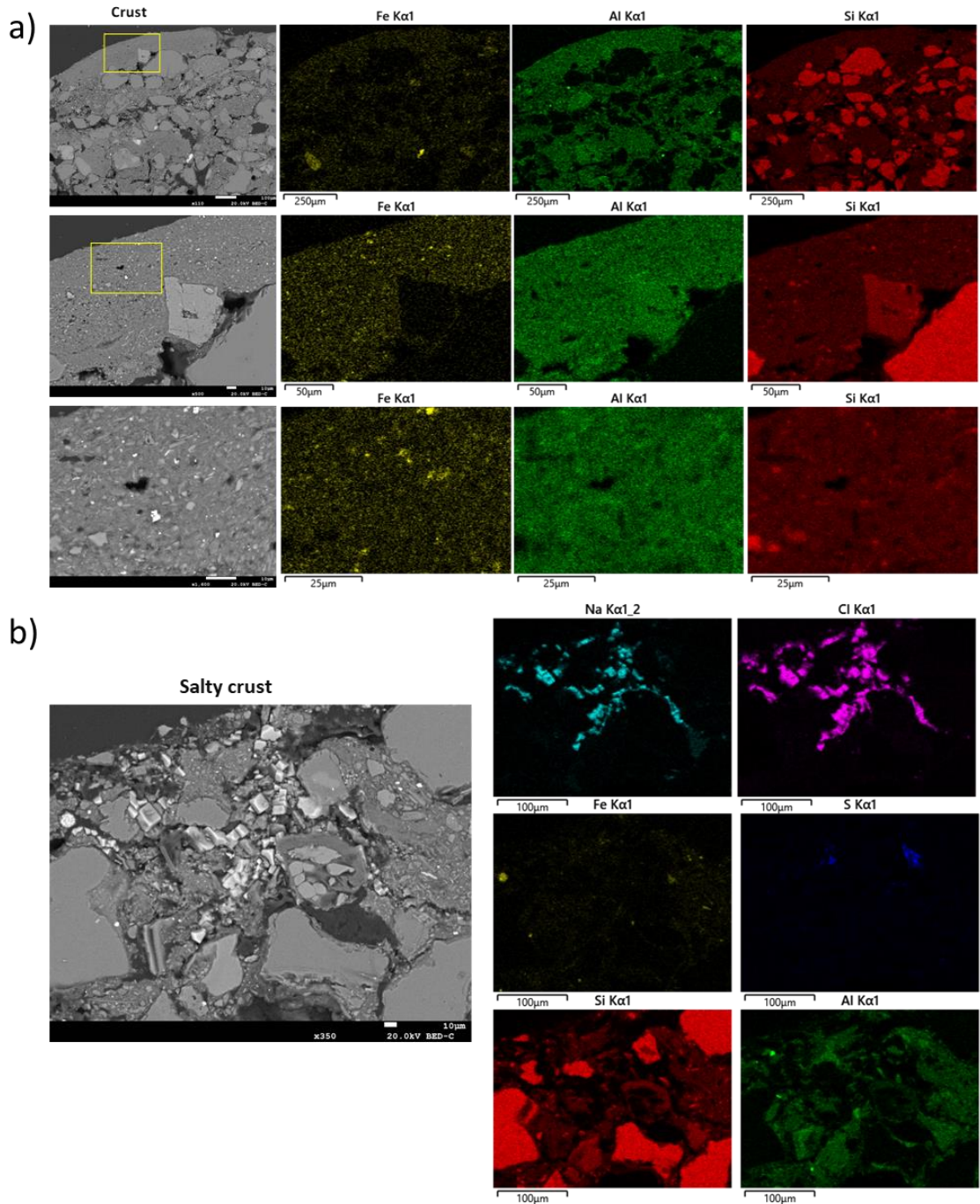


Figure S6. a) Scanning electron microscope of the top section of a crust with a zoom in on a small part, together with the elemental mapping of Fe, Al and Si with presence of homogeneous presence of iron (silicates and iron oxides). b) Detailed scanning electron microscope image and elemental mapping with Na, Cl, Fe, S, Si and Al for a very top section of a salty crust with very well formed halite crystals.

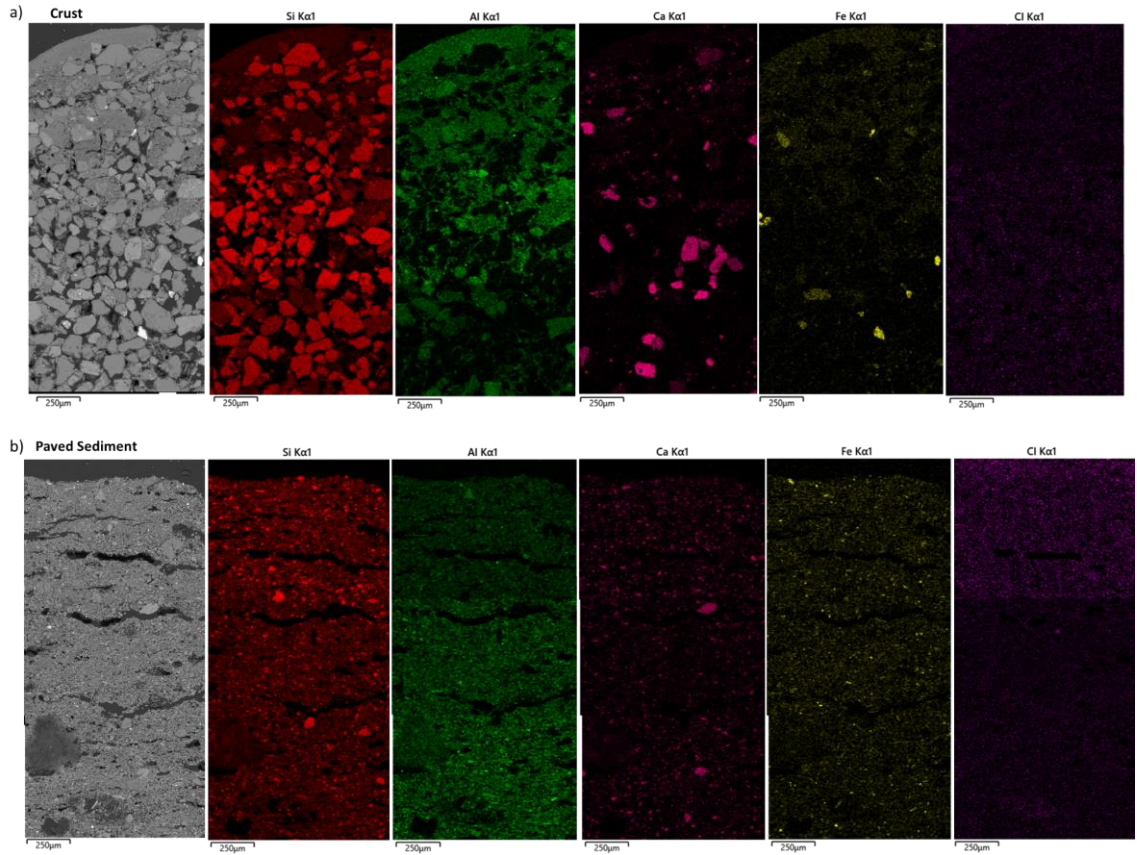


Figure S7. Crust a) and paved sediment b) profile of the first millimetres from the low-lands on the scanning electron microscope with elemental mapping of Si, Al, Ca, Fe and Cl.

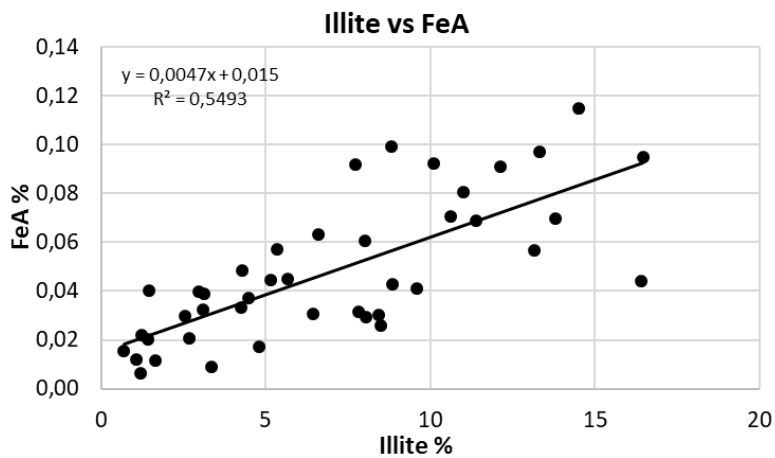


Figure S8. Correlation between most present clay (Illite) and readily exchangeable Fe (FeA).

Table S1. Sample summarize of MDPSD and FDPSD. Nº is the nº of sample, Coord. Are the coordinates of the samples, ES: Erg Smar, LB: L'Bour and HL: High-lands, MDPSD: Minimally dispersed particle size distribution and FDPSD: Fully dispersed particle size distribution.

Nº	Coord.	Coord.	Type	Location	MDPSD (μm)	FDPSD (μm)
1	29°42'800"	6°01,972'	CRUST	ES	85	9.0
2	29°42'801"	6°01,975'	CRUST	ES	84	8.5
8	29°43'607"	6°04,964'	CRUST	ES	147	5.2
11	29°43'603"	6°04,966'	CRUST	ES	21	2.9
12	29°43'604"	6°04,963'	CRUST	ES	110	6.1
14	29°45'592	5°59,585'	CRUST	ES	104	10
25	29°49,674'	5°52,436'	CRUST	LB	20	17
31	29°49,631'	5°57,335'	CRUST	HL	99	80
34	29°41,505'	6°02,872'	CRUST	ES	181	9.1
40	29°42,933	6°01,990	CRUST	ES	320	2.7
108	29°56,604	6°23,267	CRUST	HL	89	20
109	29°51,590	6°29,762	CRUST	HL	93	272
10	29°43'604"	6°04,964'	SEDIMENT	ES	147	5.8
15	29°45'592	5°59,585'	SEDIMENT	ES	83	39
19	29°49,670'	5°52,434'	SEDIMENT	LB	20	13
27	29°49,674'	5°52,436'	SEDIMENT	LB	23	18
29	29°49,649'	5°52,382'	SEDIMENT	LB	68	16
32	29°49,631'	5°57,335'	SEDIMENT	HL	97	12
49	29°49'31.53"	°52'26.09"	SEDIMENT	LB	49	16
4	29°42'800"	6°01,972'	PAVED SED	ES	25	12
7	29°42'542"	6°02,053'	PAVED SED	ES	19	8.3
9	29°43'604"	6°04,964'	PAVED SED	ES	74	5.9
16	29°45'592	5°59,585'	PAVED SED	ES	105	7.5
17	29°45'592	5°59,585'	PAVED SED	ES	94	78
18	29°49,670'	5°52,434'	PAVED SED	LB	152	5.3
35	29°41,505'	6°02,872'	PAVED SED	ES	48	19
41	29°42,933	6°01,990	PAVED SED	ES	148	6.8
42	29°42,933	6°01,990	PAVED SED	ES	31	8.1
46	29°47,196	5°56,724	PAVED SED	LB	89	67
50	29°49'31.53"	°52'26.09"	PAVED SED	LB	29	14
5	29°43'203"	6°02,171'	DUNE	ES	282	263
6	29°43'203"	6°02,171'	DUNE	ES	263	243
26	29°49,674'	5°52,436'	DUNE	LB	132	138
33	29°41,505'	6°02,872'	DUNE	ES	244	239
36	29°41,532'	6°02,900	DUNE	ES	355	308
43	29°47,196	5°56,724	DUNE	LB	159	128
44	29°47,196	5°56,724	DUNE	LB	143	132
47	29°50,049	5°52,002	DUNE	LB	192	159
48	29°49,870	5°48,318	DUNE	LB	244	272
103	29°50,927	6°2,591	DUNE	HL	195	169
104	29°50,927	6°2,591	DUNE	HL	197	268
107	29°50,791	6°12,274	DUNE	HL	243	312

Table S2. Average particle size (fully dispersed PSD, FD-PSD and minimally dispersed PSD, MD-PSD) and mineralogy of crusts in this study compared to global dust samples. Note that in this study samples are crust sediments, and in the others deposited dust.

Samples	Region	Reference	Particle size (%)				Minerals (%)		
			Silt+Clay	Sand	Quartz	Feldspars	Carbonates	Clays	Others
Crust	Morocco	Present study FD-PSD	72	28	44	8	28	17	3
Crust	Morocco	Present study MD-PSD	41	59	44	8	28	17	3
Dep. dust	Kuwait	Al-Dousari et al. 2019	63	37	38	10	45	2	5
Dep. dust	Ahwar-Iraq	Doronzo et al. 2016	97	3	13	8	80	0	0
Dep. dust	Manamah-Bahrain	Al-Dousari et al. 2019	87	12	32	10	41	3	15
Dep. dust	Walameen-South Saudi	Al-Dousari et al. 2020	61	40	62	24	13	1	0
Dep. dust	Ain-Emirates	Al-Dousari et al. 2018	4	97	26	20	52	1	0
Dep. dust	Dubai-Emirates	Subramaniam et al. 2015	82	17	21	6	45	0	27
Dep. dust	Amman-Jordan	Alshemmarri et al. 2013	70	30	21	4	68	0	7
Dep. dust	Tripoli-Libya	Al-Ghadban et al. 1999	81	20	64	5	27	4	0
Dep. dust	Cairo-Egypt	Al-Dousari et al. 2020	90	10	51	15	34	0	0
Dep. dust	Cartagena-Colombia	Doronzo et al. 2016	90	10	66	33	0	0	1
Dep. dust	Bald Hill-Australia	Cattle et al. 2002	90	9	57	2	0	14	7
Dep. dust	Average		74	26	41	12	37	2	6

Table S3. Summary of Fe mode of occurrence in weight %. Abbreviations are Nº is the number of the sample, ES: Erg Smar, LB: L'Bour, HL: Highland, FeT: total Fe, FeD: Dithionite Fe, FeA: Ascorbate Fe and FeS: structural Fe.

Nº	Type	Location	FeT	FeD	FeA	FeS
1	CRUST	ES	3.8	1.2	0.08	2.5
2	CRUST	ES	3.0	0.87	0.04	2.1
8	CRUST	ES	4.1	1.2	0.12	2.7
11	CRUST	ES	4.7	1.5	0.09	3.1
12	CRUST	ES	3.5	0.96	0.07	2.4
14	CRUST	ES	3.4	1.1	0.09	2.3
25	CRUST	LB	3.3	0.93	0.03	2.3
31	CRUST	HL	3.2	0.98	0.04	2.2
34	CRUST	ES	3.9	1.2	0.07	2.7
40	CRUST	ES	5.0	1.6	0.10	3.3
108	CRUST	HL	2.8	1.0	0.04	1.8
109	CRUST	HL	2.8	0.88	0.06	1.8
4	PAVED SEDIMENT	ES	3.5	0.99	0.04	2.4
7	PAVED SEDIMENT	ES	3.7	1.1	0.06	2.6
9	PAVED SEDIMENT	ES	3.6	0.98	0.09	2.5
16	PAVED SEDIMENT	ES	3.7	1.0	0.10	2.6
17	PAVED SEDIMENT	ES	2.4	0.59	0.03	1.8
18	PAVED SEDIMENT	LB	3.6	1.1	0.07	2.4
35	PAVED SEDIMENT	ES	2.9	0.74	0.03	2.2
41	PAVED SEDIMENT	ES	3.7	1.1	0.06	2.5
42	PAVED SEDIMENT	ES	3.9	1.2	0.06	2.6
46	PAVED SEDIMENT	LB	2.7	0.80	0.05	1.8
50	PAVED SEDIMENT	LB	3.3	1.2	0.03	2.1
10	SEDIMENT	ES	3.9	1.1	0.10	2.7
15	SEDIMENT	ES	2.4	0.65	0.04	1.7
19	SEDIMENT	LB	3.2	0.89	0.04	2.3
27	SEDIMENT	LB	3.1	0.94	0.04	2.1
29	SEDIMENT	LB	3.2	0.93	0.03	2.2
32	SEDIMENT	HL	3.2	1.1	0.03	2.1
49	SEDIMENT	LB	3.2	1.1	0.03	2.1
5	DUNE	ES	1.9	0.43	0.02	1.5
6	DUNE	ES	2.0	0.45	0.02	1.5
26	DUNE	LB	1.6	0.43	0.02	1.2
33	DUNE	ES	1.8	0.31	0.02	1.5
36	DUNE	ES	2.8	0.43	0.02	2.3
43	DUNE	LB	2.3	0.63	0.04	1.6
44	DUNE	LB	1.9	0.46	0.03	1.4
47	DUNE	LB	2.0	0.63	0.04	1.3
48	DUNE	LB	2.2	0.52	0.01	1.6
103	DUNE	HL	2.1	0.74	0.01	1.3
104	DUNE	HL	1.6	0.48	0.01	1.1
107	DUNE	HL	1.7	0.46	0.01	1.2